JACS
JOURNAL OF THE AMERICAN CHEMICAL SOCIETY

Communication

pubs.acs.org/JACS

A 2D Semiquinone Radical-Containing Microporous Magnet with Solvent-Induced Switching from T_c = 26 to 80 K

Ie-Rang Jeon, Bogdan Negru, Richard P. Van Duyne, and T. David Harris*

Department of Chemistry, Northwestern University, 2145 Sheridan Road, Evanston, Illinois 60208-3113, United States

Supporting Information

ABSTRACT: The incorporation of tetraoxolene radical bridging ligands into a microporous magnetic solid is demonstrated. Metalation of the redox-active bridging ligand 2,5-dichloro-3,6-dihydroxy-1,4-benzoquinone (LH_2) with Fe^{II} affords the solid $(Me_2NH_2)_2[Fe_2L_3]\cdot 2H_2O\cdot 6DMF$. Analysis of X-ray diffraction, Raman spectra, and Mössbauer spectra confirm the presence of Fe^{III} centers with mixed-valence ligands of the form $(L_3)^{8-}$ that result from a spontaneous electron transfer from Fe^{II} to L^{2-}. Upon removal of DMF and H_2O solvent molecules, the compound undergoes a slight structural distortion to give the desolvated phase $(Me_2NH_2)_2[Fe_2L_3]$, and a fit to N_2 adsorption data of this activated compound gives a BET surface area of 885(105) m^2/g. Dc magnetic susceptibility measurements reveal a spontaneous magnetization below 80 and 26 K for the solvated and the activated solids, respectively, with magnetic hysteresis up to 60 and 20 K. These results highlight the ability of redox-active tetraoxolene ligands to support the formation of a microporous magnet and provide the first example of a structurally characterized extended solid that contains tetraoxolene radical ligands.

The formation of extended solids that exhibit both permanent porosity and magnetic ordering represents an important synthetic challenge, as these materials may find use in applications including lightweight magnets, magnetic sensors, and the magnetic extraction of paramagnetic gases such as O_2 and NO.[1] To date, most porous magnets have featured paramagnetic metal ions connected by inorganic bridging ligands such as oxide or cyanide. While the vast majority of these compounds display magnetic ordering well below 100 K,[1d] they have been shown to order at temperatures of up to 219 K.[2] Nevertheless, the chemistry of inorganic solids is limited by an inherent lack of ligand functionalization and structural diversity, both of which are critical to systematically vary and control magnetic behavior and porosity.

In contrast, employment of organic bridging ligands to form metal-organic frameworks (MOFs) gives rise to a diverse and modular set of structures that can also exhibit high surface areas. However, the large metal−metal separations and thus weak magnetic interactions enforced by multi-atom organic bridging ligands generally leads to very low magnetic ordering temperatures, as ordering temperature is directly correlated to strength of exchange interactions.[3] In fact, the highest ordering temperature yet reported for a MOF with a well-defined surface area is only T_c = 32 K.[4] As an alternative, one can envision the use of organic radical ligands to link paramagnetic metal centers in an extended solid,[5] such that the ligand-based magnetic orbital will overlap with that of the metal to promote strong metal-radical direct exchange and, consequently, a high ordering temperature. Indeed, this approach has been extensively investigated using derivatives of nitroxide,[6] organonitrile,[7,8] perchlorotriphenylmethyl,[9] and triplet carbene radicals.[10] While magnetic solids that order even above room temperature have been synthesized with these ligands,[8a] they have not been shown to exhibit well-defined permanent porosity.

Derivatives of 2,5-dihydroxy-1,4-benzoquinone are particularly well-suited for the construction of microporous MOFs with strong magnetic coupling. These tetraoxolene ligands readily undergo redox chemistry to stabilize both diamagnetic and paramagnetic, or semiquinone, isomers. Indeed, a number of mononuclear[11] and dinuclear[12] molecular complexes containing related radical ligands have been shown to exhibit extremely strong magnetic interactions, in some cases so strong that the spin ground state is isolated even at 300 K.[13,14] In addition, these ligands have been shown to generate extended solids of varying dimensionality with large estimated void volumes, and as such could potentially give rise to materials with permanent porosity.[15−17] Despite this potential, no structurally characterized example of an extended solid that incorporates tetraoxolene radicals has been reported.

In an attempt to synthesize a semiquinone radical-containing extended solid, we targeted a system involving spontaneous electron transfer from a metal ion to a diamagnetic ligand upon solid formation. Similar electron transfer has been observed in a number of molecular transition metal complexes containing related dioxolene ligands,[18] and one-electron oxidation of dinuclear Fe^{II}_2 and Co^{II}_2 complexes bridged by tetraoxolene ligands has given radical-bridged Fe^{III}_2[12b] and Co^{III}_2[19] complexes through rearrangement of valence electrons. Herein, we report the synthesis and magnetic properties of a microporous layered solid comprised of Fe^{III} centers bridged by a radical form of chloranilic acid (LH_2 = 2,5-dichloro-3,6-dihydroxy-1,4-benzoquinone). Upon activation, the solid exhibits a surface area of 885(105) m^2/g, and its magnetic ordering temperature changes from 80 to 26 K. To our knowledge, this material represents the first structurally characterized solid incorporating a paramagnetic tetraoxolene ligand.

Reaction of $Fe(BF_4)_2\cdot 6H_2O$ with LH_2 in DMF at 130 °C under a dinitrogen atmosphere afforded shiny black, hexagonal

Received: October 4, 2015
Published: November 17, 2015

DOI: 10.1021/jacs.5b10382
J. Am. Chem. Soc. 2015, 137, 15699−15702

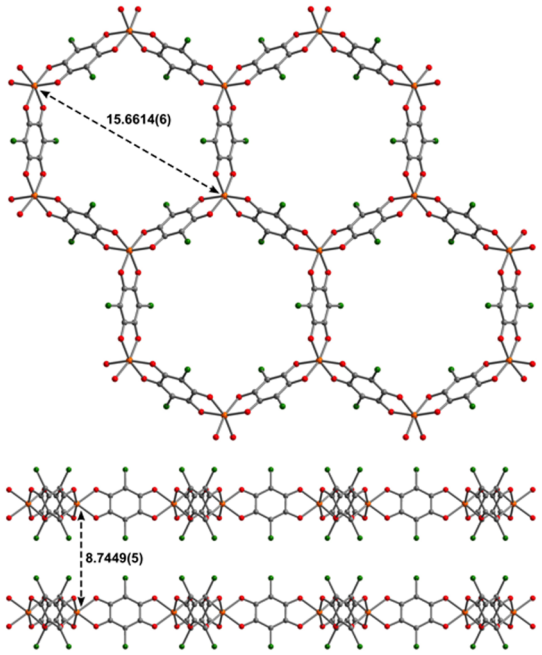

Figure 1. X-ray crystal structure of $[Fe_2L_3]^{2-}$, as viewed along the crystallographic *c* axis (upper) and *b* axis (lower), with selected Fe···Fe distances (Å). Orange = Fe, green = Cl, red = O, and gray = C.

plate-shaped crystals of $(Me_2NH_2)_2[Fe_2L_3]\cdot 2H_2O\cdot 6DMF$ (**1**). Single-crystal X-ray analysis of **1** reveals a trigonal structure featuring two-dimensional honeycomb-like layers comprised of Fe centers bridged by L^{n-}. Each Fe center resides in an octahedral coordination environment and is ligated by six O donor atoms from three different deprotonated L^{n-} ligands (see Figure 1, upper). The Fe center is situated on a site of crystallographic three-fold symmetry, with three L^{n-} ligands related in a propeller-like arrangement. The charge of the dianionic network is compensated by $Me_2NH_2^+$ ions (see Figure S1), which are generated in situ through decomposition of DMF.[20] Within **1**, the layers are eclipsed along the crystallographic *c* axis, with a H_2O molecule positioned in between Fe centers, leading to the formation of one-dimensional hexagonal channels. The channels are occupied by disordered DMF molecules, as was confirmed by microelemental analysis and thermogravimetric analysis (TGA) (see Figure S2). The structure of **1** features an intralayer Fe···Fe distance along the diagonal of the hexagonal channel of 15.6614(6) Å, with an interlayer Fe···Fe distance of 8.7449(5) Å (see Figure 1, lower). Finally, an analogous reaction of $Zn(NO_3)_2\cdot 6H_2O$ with LH_2 gave purple, hexagonal plate-shaped crystals of the isostructural compound $(Me_2NH_2)_2[Zn_2L_3]\cdot 2H_2O\cdot 6DMF$ (**2**, see Figure S3).

While compounds **1** and **2** feature isostructural dianionic networks, close inspection of bond lengths reveals several key differences. First, the mean C−C bond distance in **1** is 1.414(8) Å, 1.6% shorter than that of 1.436(7) Å found in **2**. In addition, the C−O bond distance of 1.280(6) Å in **1** is 2.9% longer than that of 1.244(5) Å in **2**. The distances in **2** are consistent with those previously reported in diamagnetic, dianionic tetraoxolene-containing honeycomb-like networks,[16] while **1** exhibits bond distances characteristic of a higher net C−C bond order and a lower net C−O bond order. Nevertheless, the mean C−C and C−O distances in **1** are still slightly longer and shorter, respectively, than those reported for semiquinone, trianionic tetraoxolene radicals in molecular complexes, which feature mean C−C and C−O distances of 1.353(3) and 1.293(3) Å, respectively.[12b] Additionally, the Fe−O distance of 2.020(3) Å is consistent with high-spin Fe^{III} ions in similar coordination environments.[21] Taken together, these structural observations suggest a configuration for the network in **1** of $[Fe^{III}_2(L_3)^{8-}]^{2-}$, a form which presumably results from a spontaneous electron transfer from Fe^{II} to L^{2-}, while the network in **2** can be described as $[Zn^{II}_2(L^{2-})_3]^{2-}$. To our knowledge, **1** represents the first structurally characterized example of any extended solid incorporating a tetraoxolene radical bridging ligand.

Upon soaking in THF and subsequent activation at 120 °C under reduced pressure, **1** can be desolvated to give $(Me_2NH_2)_2[Fe_2L_3]$ (**1a**), where complete removal of solvent molecules was confirmed by IR spectroscopy, TGA, and elemental analysis (see Figures S4 and S5 and Experimental Section). The X-ray powder diffraction pattern of **1a** exhibits a significantly different profile than that of **1** (see Figure S6). A simulation of this pattern using MOF-FIT 2.0[22] reveals a slight structural distortion of the hexagonal channels upon desolvation, accompanied by a contraction of interlayer Fe···Fe separation of 9.3% (see Figure S7). N_2 adsorption data collected at 77 K for **1a** gave a Brunauer-Emmett-Teller (BET) surface area of 885(105) m^2/g, confirming the presence of permanent microporosity (see Figure S8). This value is the second highest reported for a porous magnet, eclipsed only by a value of 1050 m^2/g reported for a lactate-bridged Co^{II} solid.[4] Finally, the structural distortion is fully reversible, as evidenced by powder X-ray diffraction, with **1a** converting back to **1** upon soaking in DMF (see Figure S6). Similar "breathing" behavior has been previously observed in a number of MOFs.[22,23]

To confirm the presence of Fe^{III} in the Fe_2L_3 solid, Mössbauer spectra were collected for **1** and **1a** (see Figure S9). At 80 K, the spectrum for **1** exhibits a sharp quadrupole doublet, and a fit to the data give an isomer shift of δ = 0.576(1) mm/s and a quadrupole splitting of ΔE_Q = 1.059(2) mm/s. These parameters can be unambiguously assigned to a high-spin Fe^{III} center.[16e,21] At 5 K, the spectrum for **1** exhibits a major sextet and a second minor doublet assigned to a small amount of Fe^{II}-containing impurity. This sextet indicates slowing down of the magnetic relaxation and suggests that **1** undergoes spontaneous magnetization at 5 K. Similarly, the spectrum collected for **1a** at 80 K exhibits a doublet that can be fit to give parameters of δ = 0.595(7) mm/s and a slightly larger quadrupole splitting of ΔE_Q = 1.103(9) mm/s, indicating presence of a high-spin Fe^{III} center. The slight increase in quadrupole splitting of **1a** compared to **1** likely stems from the local distortion of the Fe coordination sphere upon activation.

The oxidation state of the bridging ligand was further probed by Raman spectra collected for samples of **1**, **1a**, and **2** at ambient temperature (see Figure 2). Raman bands observed at 1492, 1497, and 1617 cm^{-1} for **1**, **1a**, and **2**, respectively, are assigned to the ν_{CO} stretching vibration of the bridging ligand. Based on reported literature values for related dioxolene ligands,[24] the bridging ligand in **2** can be unambiguously assigned as L^{2-}. In contrast, the ν_{CO} stretching vibration in **1** and **1a** appears slightly higher in energy than the typically observed frequency of 1425-1466 cm^{-1} for the related tetraoxolene semiquinone bridging ligands in dinuclear complexes,[14a,25] which is consistent with structural observations discussed above. Moreover, the presence of only one CO stretch in **1** suggests that the two electrons transferred from Fe^{II} in $[Fe_2L_3]^{2-}$ are delocalized over the three ligands on the Raman time scale. Additionally, the strong bands at 1364, 1364, and 1360 cm^{-1} for **1**, **1a**, and **2** are assigned to the

DOI: 10.1021/jacs.5b10382
J. Am. Chem. Soc. 2015, 137, 15699−15702

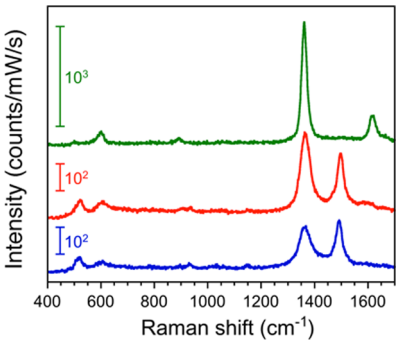

Figure 2. Raman spectra collected for solid samples of **1** (blue), **1a** (red), and **2** (green) following excitation at 405 nm.

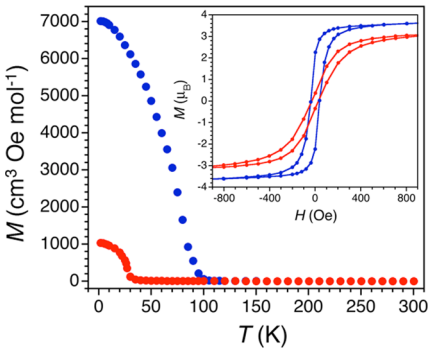

Figure 3. Variable-temperature field-cooled magnetization data for **1** (blue) and **1a** (red), collected under an applied dc field of 10 Oe. Inset: Variable-field magnetization data for **1** at 60 K (blue) and **1a** at 10 K (red).

intraligand CC vibrations, and the features at 500-600 cm^{-1} are tentatively assigned to ν_{MO} stretching modes that are coupled to the CC stretch.[26]

To investigate the magnetic behavior of **1** and **1a**, variable-temperature dc magnetic susceptibility data were collected, and the resulting plots of χ_M and $\chi_M T$ vs T for both compounds are shown in Figures S10–S12. In the case of **1**, $\chi_M T$ = 16.6 cm^3·K/mol at 300 K, which is higher than the value of 9.50 cm^3·K/mol expected for two magnetically isolated Fe^{III} centers and two $L^{3-\bullet}$ ligands, indicative of long-range strong magnetic coupling between paramagnetic centers. Upon lowering the temperature, $\chi_M T$ gradually increases and then climbs abruptly below 120 K, reflecting the increase in the magnetic correlation length within the network. Additionally, magnetic susceptibility data collected on cooling the sample with or without an applied dc field exhibit a divergence that is indicative of spontaneous magnetization. The corresponding plot of variable-temperature magnetization shows the spontaneous magnetization to occur below T = 100 K (see Figure 3).

The plot of $\chi_M T$ vs T for **1a** reveals a similar profile, albeit in a much lower temperature regime. Here, the value of $\chi_M T$ at 300 K of 9.37 cm^3·K/mol is close to that expected for two magnetically isolated Fe^{III} centers and two $L^{3-\bullet}$ ligands. The field dependence of χ_M is consistent with that observed for **1**, suggesting that the magnetic ground state is preserved upon activation (see Figure S12). However, spontaneous magnetization occurs only below T = 30 K (see Figure 3). The decrease in characteristic temperature associated with **1a** compared to **1** may stem from a decrease in coupling strength between Fe^{III} centers and $L^{3-\bullet}$ ligands due to the distortion of the framework and/or the creation of defects upon activation. Solvent-induced switching of magnetic ordering has been previously observed in both inorganic and metal-organic solids.[27] Finally, low-field remnant magnetization experiments suggest the magnetic structure of both **1** and **1a** at the characteristic temperature to approximate a dimensionality of two (see Figure S13).

To precisely determine the characteristic temperatures of **1** and **1a**, variable-temperature ac susceptibility data under zero applied field were collected at selected temperatures (see Figures S14 and S15). The data for **1** show a slightly frequency-dependent peak in both in-phase (χ_M') and out-of-phase (χ_M'') susceptibility, and give a characteristic temperature of T_c = 80 K. The frequency dependence can be quantified by the Mydosh parameter, in this case φ = 0.023, which is consistent with glassy magnetic behavior (see Supporting Information).[28] Such glassiness can result from factors such as crystallographic disorder and spin frustration arising from magnetic topology. The presence of two types of spin carrier in **1**, in conjunction with electron delocalization in the hexagonal layer, likely results in a complicated network of magnetic interactions and possibly some degree of frustration. In contrast, the plot of χ_M' vs T for **1a** exhibits a sharp, frequency-independent peak with a maximum at 26 K, indicating that **1a** undergoes long-range magnetic ordering at T_c = 26 K.

Finally, to probe the presence of magnetic hysteresis, variable-field magnetization data were collected for **1** and **1a** at selected temperatures under applied fields of up to 70 kOe (see Figure 3 inset and Figure S16). Coercive fields of H_C = 2630, 790, 150, and 40 Oe were observed for **1** at 1.8, 10, 40, and 60 K, respectively, with field-sweep rates of 4, 0.8, 0.8, and 0.8 Oe/s. The data at 1.8 K reach a value of M = 8.2 μ_B at 70 kOe, close to the value of 8 μ_B expected for antiferromagnetic coupling between two Fe^{III} ions and two $L^{3-\bullet}$ ligands. In the case of **1a**, coercive fields of H_C = 4650, 20, and 10 Oe were observed at 1.8, 10, and 20 K, respectively, with field-sweep rates of 4, 0.8, and 0.2 Oe/s. The higher H_C values observed for **1a** likely reflect the larger magnetic anisotropy engendered by structural distortion at the Fe^{III} center. Additionally, the absence of an inflection point in M vs H at temperatures close to the characteristic temperature for both compounds suggests that the interlayer interaction is negligible or ferromagnetic (see Figure S17). Taken together, these data demonstrate that **1** and **1a** behave as magnets that involve dominant intralayer antiferromagnetic interactions between adjacent spins.

The foregoing results demonstrate the incorporation of semiquinone radical ligands into an extended solid and highlight the ability of these ligands to generate a two-dimensional magnet with T_c = 80 K. Moreover, this solid exhibits permanent porosity, with its activated phase undergoing a slight structural distortion and associated decrease in magnetic ordering temperature to T_c = 26 K. Work is underway to further probe the magnetism and electrical conductivity of these solids, and to synthesize related solids that contain high-magnetic anisotropy metal ions.

■ ASSOCIATED CONTENT

Supporting Information

The Supporting Information is available free of charge on the ACS Publications website at DOI: 10.1021/jacs.5b10382.

Experimental details and characterization data, including Table S1 and Figures S1–S17 (PDF)

X-ray crystallographic files for **1** and **2** (CIF)

DOI: 10.1021/jacs.5b10382
J. Am. Chem. Soc. 2015, 137, 15699–15702

AUTHOR INFORMATION

Corresponding Author

*dharris@northwestern.edu

Notes

The authors declare no competing financial interest.

ACKNOWLEDGMENTS

This research was funded by the National Science Foundation through Grants DMR-1351959 (T.D.H.), CHE-1152547 (R.P.V.D.), and CHE-1506683 (R.P.V.D.), the Institute for Sustainability and Energy at Northwestern, and Northwestern University. Purchase of the SQUID magnetometer was supported in part by the International Institute of Nanotechnology. We thank Prof. J. T. Hupp, Prof. O. K. Farha, and C. Audu for assistance with TGA, and L. Sun for assistance using MOF-FIT 2.0.

REFERENCES

(1) (a) Maspoch, D.; Ruiz-Molina, D.; Veciana, J. *J. Mater. Chem.* **2004**, *14*, 2713. (b) Maspoch, D.; Ruiz-Molina, D.; Veciana, J. *Chem. Soc. Rev.* **2007**, *36*, 770. (c) Kurmoo, M. *Chem. Soc. Rev.* **2009**, *38*, 1353. (d) Dechambenoit, P.; Long, J. R. *Chem. Soc. Rev.* **2011**, *40*, 3249.

(2) Kaye, S. S.; Choi, H. J.; Long, J. R. *J. Am. Chem. Soc.* **2008**, *130*, 16921.

(3) Néel, L. *Ann. Phys. Paris* **1948**, *3*, 137.

(4) Zeng, M.-H.; Yin, Z.; Tan, Y.-X.; Zhang, W.-X.; He, Y.-P.; Kurmoo, M. *J. Am. Chem. Soc.* **2014**, *136*, 4680.

(5) (a) Caneschi, A.; Gatteschi, D.; Sessoli, R.; Rey, P. *Acc. Chem. Res.* **1989**, *22*, 392. (b) Vostrikova, K. E. *Coord. Chem. Rev.* **2008**, *252*, 1409. (c) Lemaire, M. T. *Pure Appl. Chem.* **2010**, *83*, 141. (d) Iwamura, H. *Polyhedron* **2013**, *66*, 3.

(6) (a) Caneschi, A.; Gatteschi, D.; Laugier, J.; Rey, P. *J. Am. Chem. Soc.* **1987**, *109*, 2191. (b) Caneschi, A.; Gatteschi, D.; Renard, J. P.; Rey, P.; Sessoli, R. *J. Am. Chem. Soc.* **1989**, *111*, 785. (c) Inoue, K.; Iwamura, H. *J. Am. Chem. Soc.* **1994**, *116*, 3173. (d) Fegy, K.; Luneau, D.; Ohm, T.; Paulsen, C.; Rey, P. *Angew. Chem., Int. Ed.* **1998**, *37*, 1270. (e) Caneschi, A.; Gatteschi, D.; Lalioti, N.; Sessoli, R.; Venturi, G.; Vindigni, A.; Rettori, A.; Pini, M. G.; Novak, M. A. *Angew. Chem., Int. Ed.* **2001**, *40*, 1760. (f) Numata, Y.; Inoue, K.; Baranov, N.; Kurmoo, M.; Kikuchi, K. *J. Am. Chem. Soc.* **2007**, *129*, 9902.

(7) (a) Zhao, H.; Heintz, R. A.; Ouyang, X.; Dunbar, K. R.; Campana, C. F.; Rogers, R. D. *Chem. Mater.* **1999**, *11*, 736. (b) Clérac, R.; O'Kane, S.; Cowen, J.; Ouyang, X.; Heintz, R.; Zhao, H.; Bazile, M. J., Jr.; Dunbar, K. R. *Chem. Mater.* **2003**, *15*, 1840. (c) Motokawa, N.; Miyasaka, H.; Yamashita, M.; Dunbar, K. R. *Angew. Chem., Int. Ed.* **2008**, *47*, 7760.

(8) (a) Manriquez, J. M.; Yee, G. T.; McClean, R. S.; Epstein, A. J.; Miller, J. S. *Science* **1991**, *252*, 1415. (b) Zhang, J.; Ensling, J.; Ksenofontov, V.; Gütlich, P.; Epstein, A. J.; Miller, J. S. *Angew. Chem., Int. Ed.* **1998**, *37*, 657. (c) Pokhodnya, K. I.; Bonner, M.; Her, J.-H.; Stephens, P. W.; Miller, J. S. *J. Am. Chem. Soc.* **2006**, *128*, 15592.

(9) Maspoch, D.; Ruiz-Molina, D.; Wurst, K.; Domingo, N.; Cavallini, M.; Biscarini, F.; Tejada, J.; Rovira, C.; Veciana, J. *Nat. Mater.* **2003**, *2*, 190.

(10) Koga, N.; Ishimaru, Y.; Iwamura, H. *Angew. Chem., Int. Ed. Engl.* **1996**, *35*, 755.

(11) (a) Kahn, O.; Prins, R.; Reedijk, J.; Thompson, J. S. *Inorg. Chem.* **1987**, *26*, 3557. (b) Bencini, A.; Carbonera, C.; Dei, A.; Vaz, M. G. F. *Dalton Trans.* **2003**, 1701.

(12) (a) Dei, A.; Gatteschi, D.; Pardi, L.; Russo, U. *Inorg. Chem.* **1991**, *30*, 2589. (b) Min, K. S.; DiPasquale, A. G.; Golen, J. A.; Rheingold, A. L.; Miller, J. S. *J. Am. Chem. Soc.* **2007**, *129*, 2360.

(13) (a) Buchanan, R. M.; Kessel, S. L.; Downs, H. H.; Pierpont, C. G.; Hendrickson, D. N. *J. Am. Chem. Soc.* **1978**, *100*, 7894. (b) Benelli, C.; Dei, A.; Gatteschi, D.; Güdel, H. U.; Pardi, D. I. *Inorg. Chem.* **1989**, *28*, 3089. (c) Wheeler, D. E.; McCusker, J. K. *Inorg. Chem.* **1998**, *37*, 2296. (d) Chang, H.-C.; Ishii, T.; Kondo, M.; Kitagawa, S. *J. Chem. Soc., Dalton Trans.* **1999**, 2467. (e) Chłopek, K.; Bothe, E.; Neese, F.; Weyhermüller, T.; Wieghardt, K. *Inorg. Chem.* **2006**, *45*, 6298.

(14) (a) Guo, D.; McCusker, J. K. *Inorg. Chem.* **2007**, *46*, 3257. (b) Jeon, I.-R.; Park, J. G.; Xiao, D. J.; Harris, T. D. *J. Am. Chem. Soc.* **2013**, *135*, 16845.

(15) Kitagawa, S.; Kawata, S. *Coord. Chem. Rev.* **2002**, *224*, 11.

(16) (a) Weiss, A.; Riegler, E.; Robl, C. *Z. Naturforsch.* **1986**, *41b*, 1501. (b) Abrahams, B. F.; Coleiro, J.; Hoskins, B. F.; Robson, R. *Chem. Commun.* **1996**, 603. (c) Abrahams, B. F.; Coleiro, J.; Ha, K.; Hoskins, B. F.; Orchard, S. D.; Robson, R. *J. Chem. Soc., Dalton Trans.* **2002**, 1586. (d) Luo, T.-T.; Liu, Y.-H.; Tsai, H.-L.; Su, C.-C.; Ueng, C.-H.; Lu, K.-L. *Eur. J. Inorg. Chem.* **2004**, *2004*, 4253. (e) Shilov, G. V.; Nikitina, Z. K.; Ovanesyan, N. S.; Aldoshin, S. M.; Makhaev, V. D. *Russ. Chem. Bull.* **2011**, *60*, 1209. (f) Atzori, M.; Benmansour, S.; Espallargas, G. M.; Clement-León, M.; Abhervé, A.; Gómez-Claramunt, P.; Coronado, E.; Artizzu, F.; Sessini, E.; Deplano, P.; Serpe, A.; Mercuri, M. L.; Gómez-García, C. J. *Inorg. Chem.* **2013**, *52*, 10031. (g) Abhervé, A.; Clement-León, M.; Coronado, E.; Gómez-García, C. J.; Verneret, M. *Inorg. Chem.* **2014**, *53*, 12014.

(17) Abrahams, B. F.; Hudson, T. A.; McCormick, L. J.; Robson, R. *Cryst. Growth Des.* **2011**, *11*, 2717.

(18) (a) Pierpont, C. G. *Coord. Chem. Rev.* **2001**, *216-217*, 99. (b) Shultz, D. A. Valence Tautomerism in Dioxolene Complexes of Cobalt. In *Magnetism: Molecules to Materials II*; Miller, J. S., Drillon, M., Eds.; Wiley-VCH: New York, 2001; Vol. 2, pp 281−306. (c) Boskovic, C. Valence Tautomeric Transitions in Cobalt-dioxolene Complexes. In *Spin-Crossover Materials: Properties and Applications*; Halcrow, M. A., Ed.; Wiley-VCH: Oxford, UK, 2013; Ch 7.

(19) (a) Carbonera, C.; Dei, A.; Létard, J.-F.; Sangregorio, C.; Sorace, L. *Angew. Chem., Int. Ed.* **2004**, *43*, 3136. (b) Tao, J.; Maruyama, H.; Sato, O. *J. Am. Chem. Soc.* **2006**, *128*, 1790. (c) Min, K. S.; DiPasquale, A. G.; Rheingold, A. L.; White, H. S.; Miller, J. S. *J. Am. Chem. Soc.* **2009**, *131*, 6229.

(20) (a) Wang, X.-F.; Zhang, Y.-B.; Cheng, X.-N.; Chen, X.-M. *CrystEngComm* **2008**, *10*, 753. (b) Zhang, J.; Chen, S. M.; Nieto, R. A.; Wu, T.; Feng, P. Y.; Bu, X. H. *Angew. Chem., Int. Ed.* **2010**, *49*, 1267. (c) Yi, F.-Y.; Jiang, H.-L.; Sun, Z.-M. *Chem. Commun.* **2015**, *51*, 8446.

(21) Nagayoshi, K.; Kabir, M. K.; Tobita, H.; Honda, K.; Kawahara, M.; Katada, M.; Adachi, K.; Nishikawa, H.; Ikemoto, I.; Kumagai, H.; Hosokoshi, Y.; Inoue, K.; Kitagawa, H.; Kawata, S. *J. Am. Chem. Soc.* **2003**, *125*, 221.

(22) Sun, L.; Hendon, C. H.; Minier, M. A.; Walsh, A.; Dincă, M. *J. Am. Chem. Soc.* **2015**, *137*, 6164.

(23) (a) Barthelet, K.; Marrot, J.; Riou, D.; Feréy, G. *Angew. Chem., Int. Ed.* **2002**, *41*, 281. (b) Feréy, G.; Serre, C. *Chem. Soc. Rev.* **2009**, *38*, 1380. (c) Murdock, C. R.; Hughes, B. C.; Lu, Z.; Jenkins, D. M. *Coord. Chem. Rev.* **2014**, *258-259*, 119.

(24) Vlček, A. *Comments Inorg. Chem.* **1994**, *16*, 207.

(25) Baum, A.; Lindeman, S. V.; Fiedler, A. T. *Chem. Commun.* **2013**, *49*, 6531.

(26) (a) Hartl, F.; Stufkens, D. J.; Vlček, A. *Inorg. Chem.* **1992**, *31*, 1687. (b) Holt, B. T. O.; Vance, M. A.; Mirica, L. M.; Heppner, D. E.; Stack, T. D. P.; Solomon, E. I. *J. Am. Chem. Soc.* **2009**, *131*, 6421.

(27) (a) Larionova, J.; Chavan, S. A.; Yakhmi, J. V.; Frøystein, A. G.; Sletten, J.; Sourisseau, C.; Kahn, O. *Inorg. Chem.* **1997**, *36*, 6374. (b) Kurmoo, M.; Kumagai, H.; Hughes, S. M.; Kepert, C. J. *Inorg. Chem.* **2003**, *42*, 6709. (c) Nelson, K. J.; Giles, I. D.; Troff, S. A.; Arif, A. M.; Miller, J. S. *Inorg. Chem.* **2006**, *45*, 8922. (d) Yanai, N.; Kaneko, W.; Yoneda, K.; Ohba, M.; Kitagawa, S. *J. Am. Chem. Soc.* **2007**, *129*, 3496. (e) Milon, J.; Daniel, M.-C.; Kaiba, A.; Guionneau, P.; Brandes, S.; Sutter, J.-P. *J. Am. Chem. Soc.* **2007**, *129*, 13872. (f) Cheng, X.-N.; Zhang, W.-X.; Chen, X.-M. *J. Am. Chem. Soc.* **2007**, *129*, 15738. (g) Ohkoshi, S.; Tsunobuchi, Y.; Takahashi, H.; Hozumi, T.; Shiro, M.; Hashimoto, K. *J. Am. Chem. Soc.* **2007**, *129*, 3084. (h) Duan, Z.; Zhang, Y.; Zhang, B.; Zhu, D. *J. Am. Chem. Soc.* **2009**, *131*, 6934. (i) Motokawa, N.; Matsunaga, S.; Takaishi, S.; Miyasaka, H.; Yamashita, M.; Dunbar, K. R. *J. Am. Chem. Soc.* **2010**, *132*, 11943.

(28) Mydosh, J. A. *Spin Glasses*; Taylor & Francis: London/Washington, DC, 1993.

DOI: 10.1021/jacs.5b10382
J. Am. Chem. Soc. 2015, 137, 15699−15702